Supporting information for

Growth mechanism of CH_3NH_3I in a vacuum processed perovskite

Beom-Soo Kim[a], Yoonjay Han[a] and Jang-Joo Kim[a,b]*

[a] *Department of Materials Science and Engineering, Seoul National University, Seoul, 151-742, South Korea*

[b] *Research Institute of Advanced Materials (RIAM), Seoul National University, Seoul, 151-744, South Korea*

E-mail: jjkim@snu.ac.kr

Methods

Film fabrication

The ITO-coated glass were cleaned with acetone and isopropyl alcohol. The 20 nm of C_{60} (SES research) NPB (Nichem) and Au(iTASCO) and PbI_2 (Alpha Aesar) were deposited on the ITO substrate. On the substrates, MAI (2 times purified by sublimation graded, Jida Rubibo Optoelectronic Tech) was heated until it reaches 7×10^{-5} torr, monitored by ionization gauge (Varian 572, Agilent Technologies) for the desired times. For the films of MAI/PbI_2 (*x* nm), the 2, 20, 100 and 200 nm of PbI_2 layers were deposited on the ITO substrate and then the MAI was exposed to the substrates for 0, 10, 20 30 and 60 minutes. For the accurate control the MAI, the same amount MAI source, 1.50 g, was carefully measured and loaded in a crucible

through a nitrogen-filled glove box. The PbI_2 was previously calibrated by thickness monitor and measuring the deposited film thickness from surface profilometer (KLA-Tencor Alpha-Step IQ). Before the deposition of MAI, the source was pre-heated at 45℃ in ~20 minutes for the out gassing from the source and warming up the crucible. The temperature was controlled by PID control (SJ Power, STP-1500) and from the time reaching the desired working pressure, the temperature was manually controlled to maintain the working pressure constant.

QCM analysis

The QCMs (INFICON, 5 MHz) were monitored by crystal oscillation type deposition controller, (CRTM-9000, ULVAC). When the bare QCMs were loaded for the two sensor positions, the MAI was deposited and it was calibrated to read same thickness by adjusting the tooling factor for sensor 1 from 1.000 (default value) to 0.877 from the thickness difference. The other deposition parameters such as Z-ratio and density remained same (Z-ratio=1, density=1g/cm^3). The PbI_2 layers were deposited ~1 Å/s under 1×10^{-6} torr only on the sensor 2. The two sensors, exposed to MAI at the same. The deposited weights are extracted from the monitored thicknesses using equation $\Delta f = C_f \Delta m$ where Δf is frequency change, C_f is sensitivity factor for 5 MHz AT-cut quartz crystal, 56.6 Hzμg^{-1}cm^2 and Δm is mass weight change per unit area, (g/cm^2). In our experiment, the $\Delta f/f < 0.005$, therefore it is able to apply the equation above assuming the variation from z ratio is negligible [1].

Characterization

The thicknesses of the films measured by a profilometry (KLA-Tencor Alpha-Step IQ). The films are scratched by surgical blade and then step heights were measured (Fig. S1). X-ray diffraction (XRD) measurements were carried out by D8 Advance diffractometer (Bruker)

using Cu Ka radiation. The steps were 0.04 degree with exposure time for 1 second for each step. The topology, phase and surface potential images were measured by the XE-100 (Park systems) integrated with lock in amplifier (SR830, Stanford Research Systems) under ambient condition at room temperature using Pt/Cr-coated ElectriTap300g (Budget sensors). The SKPM measurement were carried out in non-contact mode with scan parameters as V_{AC}=2 V, resonance frequency of 17 kHz and scan rate for 0.5 Hz. All of the images were measured at least 3 times with different scales to extract the statistical information of the surface such as root mean square roughness and surface potential values.

Assignment of XRD peaks (Fig. 1b)

The peak at 12.7° and 25.6° corresponds to PbI_2 (001) and (002). The peaks at 14.2, 28.2°, 28.5°, 31.7°, 40.5° and 43.1° correspond to (110) (004) (220) (310) (224) and (314) of tetragonal phase $CH_3NH_3PbI_3$ perovskite. The peaks at 19.7°, 19.9° and 26.3° correspond to (002), (101) and (102) CH_3NH_3I [2].

Supporting figures

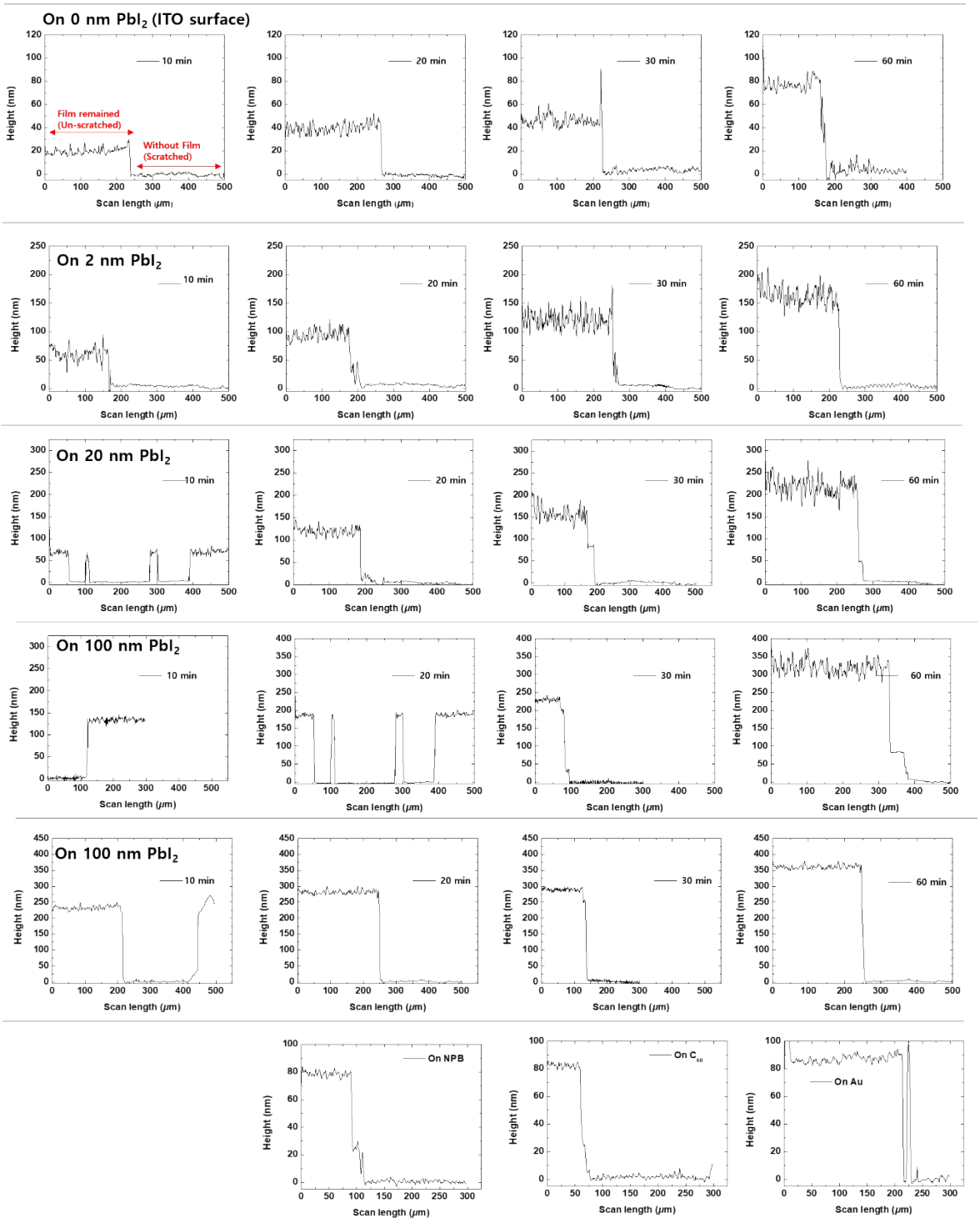

Fig. S1. The scan profiles measured by stylus profilometer for the thicknesses of the films

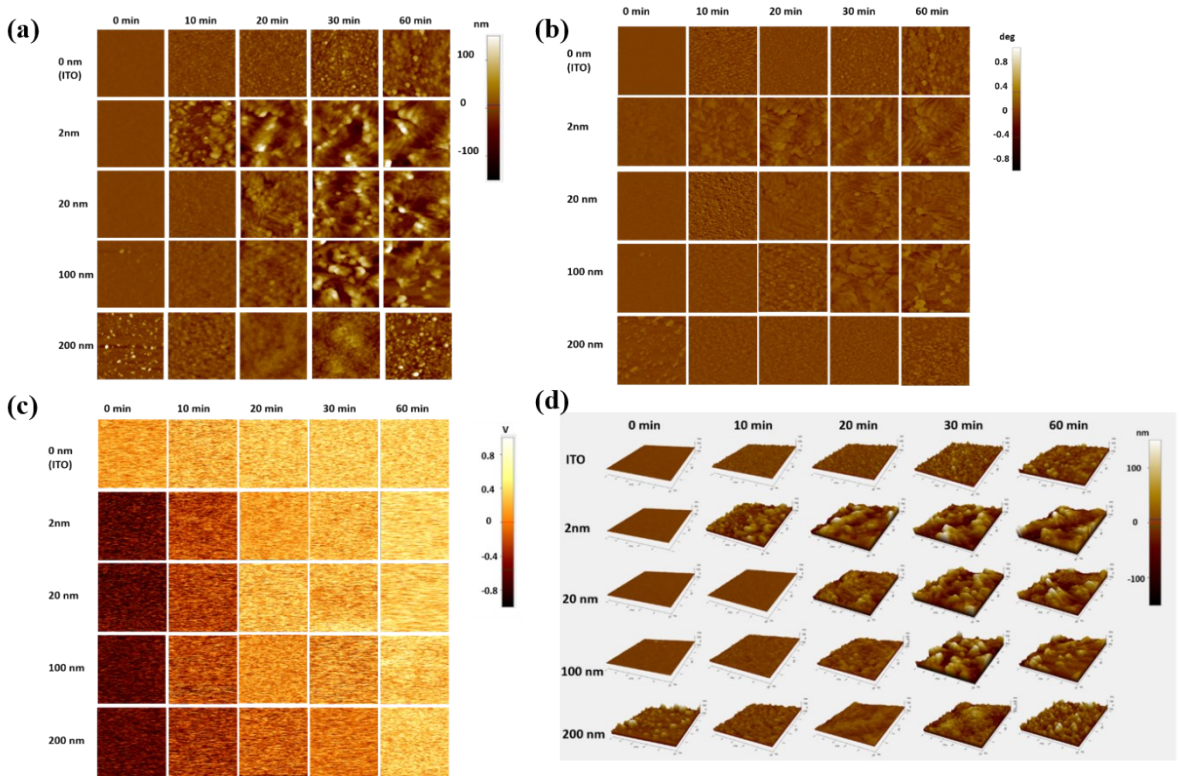

Fig. S2 (a) Topology (b) phase and (c) surface potentials of the films shown in Fig. 3 with $5\ \mu m \times 5\ \mu m$ scale. (d) 3-d image for the topology for the same scale.

Table S1. The root mean square roughness of the films shown in Fig. 3.

Initial PbI_2 thickness / MAI exposure time	0 nm (ITO)	2 nm	20 nm	100 nm	200 nm
0 min.	1.7	1.7	1.7	4.5	23.1
10 min.	7.9	28.2	2.5	6.5	10.2
20 min.	11.1	33.7	24.3	15.8	11.6
30 min.	20.0	37.3	36.0	41.0	22.3
60 min.	20.1	37.3	39.2	45.5	30.1

*unit: nm

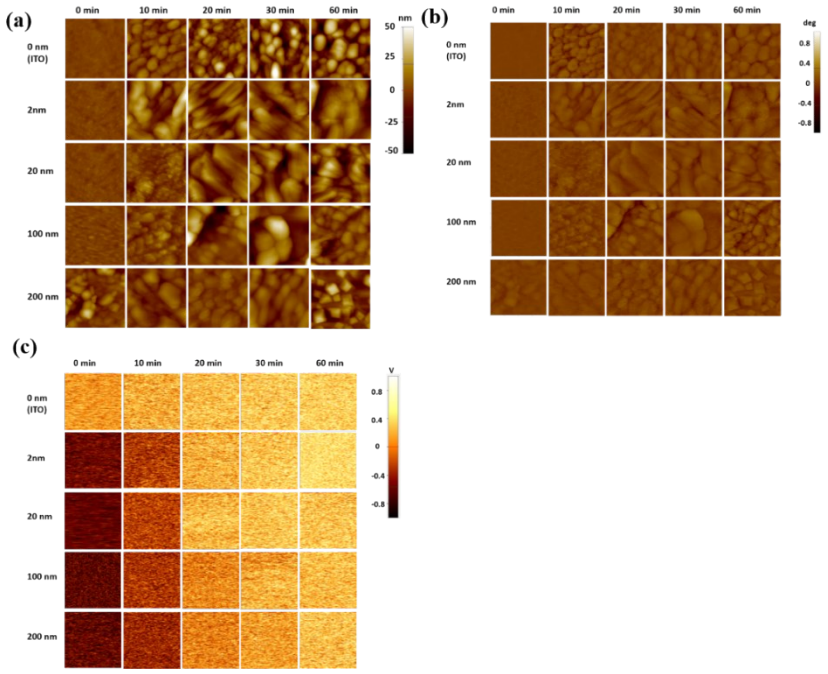

Fig. S3 (a) Topology (b) phase and (c) surface potentials of the films shown in Fig. 3 with 1 $\mu m \times 1\ \mu m$ scale

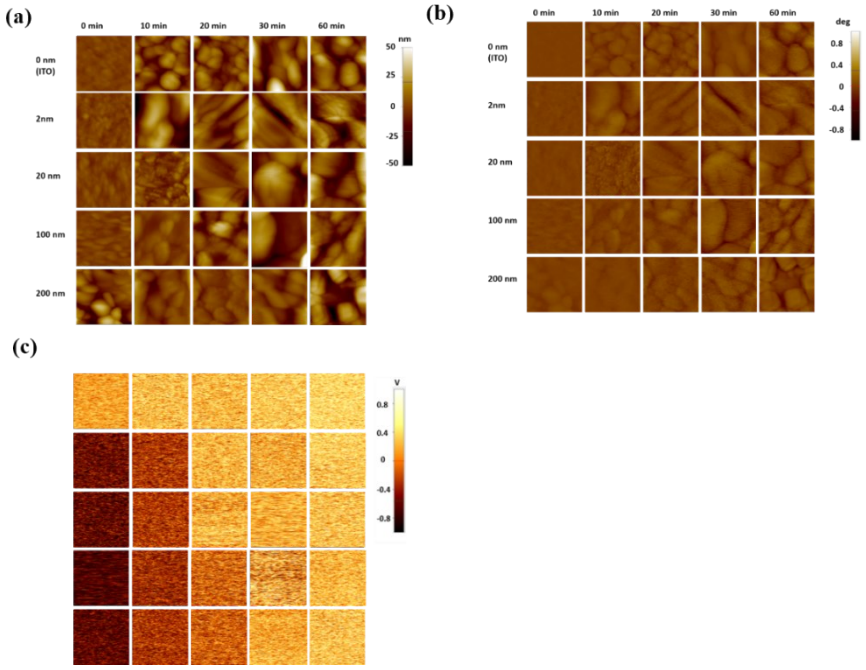

Fig. S4 (a) Topology (b) phase and (c) surface potentials of the films shown in Fig. 3 with 0.5 $\mu m \times 0.5\ \mu m$ scale

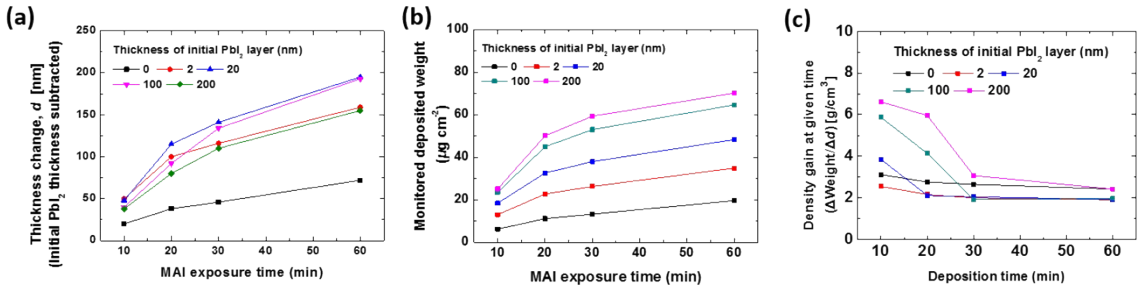

Fig. S5 (a) Thickness change of the films (b) deposited weight and (c) density of the deposited film (deposited weight over thickness change at given times). The deposited weights are measured by the QCMs shown in Fig. 2b.

Density of the deposited films

Fig. S5a shows the thicknesses (d) of the deposited films measured by profilometry after subtraction the initial thickness of PbI_2. Fig. S4b is the monitored deposited weights, w, measured by QCM shown in fig. 2c. Fig. S4c shows the values for deposited weight change, $w_{t_n} - w_{t_{n+1}}$, shown in Fig. S4b, where t_n=t_0, t_1, t_2 t_3 and t_4 correspond to t=0, 10, 20, 30 and 60 minutes respectively, divided by thickness change, $d_{t_n} - d_{t_{n+1}}$, in the unit of g/cm^3. The reported density for MAI, PbI_2 and the $MAPbI_3$ are 2.22, 6.16 and 4.15 g/cm^3 respectively [3-5].

References

[1] Srivastava, A. K.; Sakthivel, P. *J. Vac. Sci. Technol., A* **2001**, 19, 97−100

[2] Chen, X.; Myung, Y.; Thind, A.; Gao, Z.; Yin, B.; Shen, M.; Cho, S. B.; Cheng, P.; Sadtler, B.; Mishra, R.; Banerjee, P. *J. Mater. Chem. A* **2017**, 5, 24728– 24739

[3] Teuscher, J.; Ulianov, A.; Müntener, O.; Grätzel, M.; Tetreault, N. *ChemSusChem* **2015,** 8, 3847−3852.

[4] Yamamuro, O.; Oguni, M.; Matsuo, T.; Suga, H. J. *Chem. Thermodyn*., **1986**, 18, 939

[5] Huang, J.; Jiang, K.; Cui, X.; Zhang, Q.; Gao, M.; Su, M.; Yang, L.; Song, Y. *Sci. Rep*. **2015**, 5, 15889.